Hindawi
International Journal of Aerospace Engineering
Volume 2024, Article ID 8648996, 13 pages
https://doi.org/10.1155/2024/8648996

Research Article

Research on the Simulation Method for Equivalent Stiffness of Bolted Connection Thin Plate Structures

Zhe Chen,[1] **Qi-jun Zhao**,[1] **and Guo-chen Zhou**[2]

[1]*National Key Laboratory of Rotorcraft Aeromechanics, Nanjing University of Aeronautics and Astronautics, Nanjing 210016, China*
[2]*Aviation Industry Changhe Aircraft Industry (Group) Co., Ltd, Jingdezhen 333001, China*

Correspondence should be addressed to Zhe Chen; chenzhe617@163.com

Received 14 January 2023; Revised 29 May 2023; Accepted 21 June 2023; Published 26 March 2024

Academic Editor: Chuang Liu

Bolted connections are widely used in assembly structures, and their dynamic characteristics are often affected by stiffness, damping, excitation, and other factors. In order to solve the problems of low computational efficiency of fine modeling and large computational error of linearized equivalent modeling of bolted structures, this paper proposes a dynamic characteristic parameter identification method for bolted structures based on the multiscale method and considering the influence of nonlinear factors. In this method, the bolted connection characteristics are simulated in the form of a combination of shear stiffness, torsional stiffness, nonlinear stiffness, and viscous damping coefficient and identified according to the test measurement frequency and frequency response function. At the same time, by establishing the nonlinear dynamic model of bolted structure, the influence of different bolt preloads and excitation forces on the dynamic characteristics of bolted structure is studied.

1. Introduction

Bolted joints are widely used in assembled structures, where the dynamics are often influenced by various factors such as stiffness, damping, and excitation, making direct measurement of the relevant parameters very difficult [1, 2]. For example, the bolt joint surface can cause local stiffness and damping discontinuities in the structure, and the contact stiffness resulting from nonlinear contact on the bolt joint surface will also directly affect the mechanical properties of the bolt joint structure. In addition, the analytical solution for contact stiffness is often difficult to obtain or has considerable uncertainty due to factors such as contact surface area, coefficient of friction, and roughness. On the other hand, in practical engineering calculations, a certain degree of dynamical simplification or linear equivalence is usually applied to the bolt joints, and this treatment ignores the nonlinear nature of the bolt joints and fails to describe the complex nonlinear phenomena caused by the presence of the joint interface.

In the early stage, the dynamic model of the whole machine structure was composed of simple beams, bars, and plates due to the limitation of computational capacity, and the whole machine structure model only included hundreds of degrees of freedom [3]. At this stage, the dynamic model calculation results depend on the experience of the modeler, and a lot of simplification needs to be introduced in the modeling process. The established model can only roughly reflect the overall dynamic characteristics of the structure and cannot directly analyze the local deformation or dynamic stress state of the structure through the whole machine model. In addition, the calculation accuracy of the model is not satisfactory because of the introduction of a large number of simplified assumptions.

With the development of computer performance and finite element technology, dynamic modeling technology has entered the stage of fine modeling. With very detailed finite element models, researchers can obtain highly accurate calculation results, such as stress analysis, modal characteristics. However, the calculation scale of the refined model is

relatively large. For the part-level structure, it is feasible to accurately determine the mechanical properties of the part structure through this refined model. For the assembly-level structure with many parts, if the refined model is adopted, the calculation cost is still very high. Therefore, from the perspective of considering the calculation accuracy and efficiency of the model, the basic stressed structure should be properly simplified while retaining its main mechanical characteristics, which can not only meet the requirements of high-precision calculation but also control the overall model calculation scale within a reasonable range.

In general, when dealing with dynamic problems with connected structures, the commonly used method is based on the linearization idea, ignoring the connection or equivalent connection to the combination of linear spring and linear damping unit, and then using model modification, test identification, and other methods to give the parameters of the spring units and damping units. There are mainly two ways to achieve this. One is to identify the damping matrix and stiffness matrix of the connection part by using the substructure method and using the modal parameter identification method, combining the modal data or frequency response function before and after installation [4]. However, it is difficult to accurately measure the frequency response function, especially when it involves the degree of freedom of rotation. Measuring noise level is also one of the important standards to measure the recognition effect of this method, and how to reduce the error caused by environmental noise is also a difficulty of this method [5]. The other method is to simulate the connection relationship of connection parts by equivalent elements. Ahmadian et al. [6] simulates the connection of the joint surface by constructing a hexahedral isoperimetric solid element and identifying the elastic modulus and shear modulus of the element to obtain the equivalent stiffness of the connection. Kuanmi et al. [7] proposed a general form of connection element for bolted connection structures, considering the coupling between each degree of freedom of the joint surface and the connection structure, and carried out experimental verification. The experimental results show the effectiveness and reliability of this method, and the error between the identified model calculation results and the experimental results is within 10% [8]. However, this linearized equivalence ignores the nonlinear characteristics of the connection and simply simulates the effects of complex viscous sliding and clearance collision with linearized stiffness and damping, which makes this method must be based on tests and cannot meet the requirements of dynamic calculation and analysis for design. In fact, in the actual structure, most of the joint structures will show nonlinear characteristics, so it is important to study the nonlinear dynamic modeling of the joint structures. Jalali et al. [9] considered the nonlinear characteristics of the bolted interface, deduced the dynamic differential equation of the element, and used the force state mapping method to identify the mechanical property parameters of the nonlinear interface. By analogy to the linear equivalent element method, some scholars introduced nonlinear materials to simulate the nonlinear characteristics of nonlinear joint surfaces. Iranzad and Ahmadian [10] introduced elastic-plastic materials to simulate the microslip and transverse macroslip phenomena that may occur on the bolt joint surface and established the dynamic model of the joint surface using the QUAD4 element. By identifying the hardening modulus, linear modulus, yield stress, and other parameters of elastoplastic materials, the joint surface of the bolt structure can be identified. Mayer and Gaul [11] introduced the Masing damping model which can describe plastic sliding stiffness and stuck linear stiffness, used a zero-thickness contact element to simulate microsliding effect and friction in bolts, and took a specific bolt installation structure as an example to verify that the proposed connection model can well simulate the nonlinear stiffness and damping characteristics caused by bolt connection.

In this manuscript, a linearized equivalence method for the stiffness of bolted joints and an equivalence calculation method that considers nonlinear influences are proposed. Firstly, the calculation method of nonlinear contact is introduced. Secondly, the linear equivalent of bolt connection stiffness and the equivalent calculation method considering nonlinear influence factors are given, respectively. Finally, the accuracy of the two equivalent methods and their influence on the calculation accuracy are compared through numerical simulation examples.

2. Linearized Equivalent Modelling and Stiffness Calculation Method for Bolted Joint Structures

Depending on the different engineering and computational requirements, there are three main methods of linearized modelling of bolted joint structures in common: the virtual material method, the multipoint constraint method, and the spring damping method. In this manuscript, the spring damping method is mainly investigated.

When using the spring damping method to simulate bolted joints, realistic and reliable stiffness and damping inputs are the key to accurate simulation. Due to the fact that the bolts themselves are usually made of alloy steel and the form of assembly in the actual structure, the influence of damping is normally unconsidered.

According to Figure 1, the forces and the external loads on the bolts and the coupled parts are

$$\begin{cases} F_b = F_0 + K_b\delta, \\ F_m = F_0 - K_m\delta, \\ F_e = F_b - F_m = (K_b + K_m)\delta, \end{cases} \tag{1}$$

where F_b is the pressure on the bolt, F_m is the pressure on the coupling, F_0 is the initial preload, F_e is the external load, K_b is the axial stiffness of the bolt, K_m is the axial stiffness of the coupling, and δ is the deflection.

Then the equivalent stiffness of the bolted joints structure is

$$K_e = F_e/\delta = K_b + K_m. \tag{2}$$

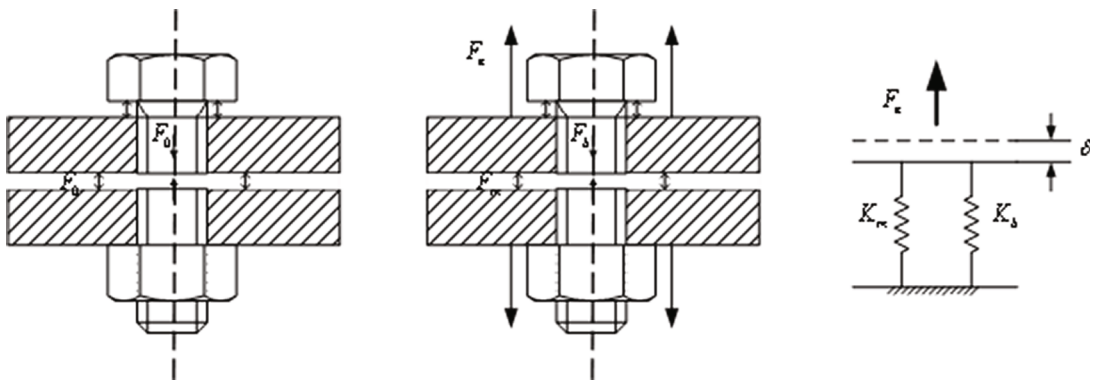

Figure 1: Stiffness model for bolted joint structures.

According to the mechanical design manual, the calculation of the bolt's own stiffness can be simplified in the form of Figure 2.

The bolt stiffness can be expressed as

$$K_b = \left(\frac{l_b + l_h}{A_b E_b} + \frac{l_t + l_{tm}}{A_s E_b}\right)^{-1}, \tag{3}$$

where A_b is the cross-sectional area of the light bar of the bolt, A_s is the equivalent cross-sectional area of the bolt, l_h is the equivalent length of the head of the bolt, l_b is the equivalent length of the light bar of the bolt, l_t is the equivalent length of the screw, and l_{tm} is the equivalent length of the screwed-in threaded section.

As shown in Figure 3, when the material thickness of the jointed parts is the same, the stiffness of the force area of the jointed parts can be expressed as [12]

$$K_m = \pi d_h \tan\theta \left[2 \ln\left(\frac{d_w + 3d_h}{d_w - d_h}\frac{d_w + L\tan\theta - d_h}{d_w + L\tan\theta + 3d_h}\right)\right]^{-1}, \tag{4}$$

where d is the nominal diameter of the bolt, d_h is the diameter of the bolt hole, direct support surface of the bolt head, and d_w is the total thickness of the part to be connected, and the half-top angle θ is calculated as

$$\theta = \alpha_1 \frac{\ln(L/d)}{\ln(R + 1/R - 1)} + \alpha_2 (C/d) + \alpha_3 \ln(L/d) + \alpha_4 \ln(R + 1/R - 1) + \alpha_5, \tag{5}$$

where $\alpha_1 = 2.5^o$, $\alpha_2 = -14^o$, $\alpha_3 = 2^o$, $\alpha_4 = -0.2^o$, and $\alpha_5 = 30^o$, and L/d is the relative total thickness; C/d is the relative clearance; R is the thickness ratio of the jointed parts.

3. Parameter Identification of Bolted Joint Structures considering Nonlinear Factors

3.1. Nonlinear Model for Bolted Beam Structures. Considering the bolted beam structure shown in Figure 4, consisting of two identical linear Euler-Bernoulli beams bolted together, with the bolted beam combination is solidly supported at both ends. Where K_l and K_θ denote the linear shear and torsional stiffnesses, respectively, K_3 denotes the cubic stiffness term, and C denotes the viscous damping factor at the joint. In this manuscript, the nonlinear spring is used to simulate the nonlinear characteristics of the contact interface under the preload of the bolts.

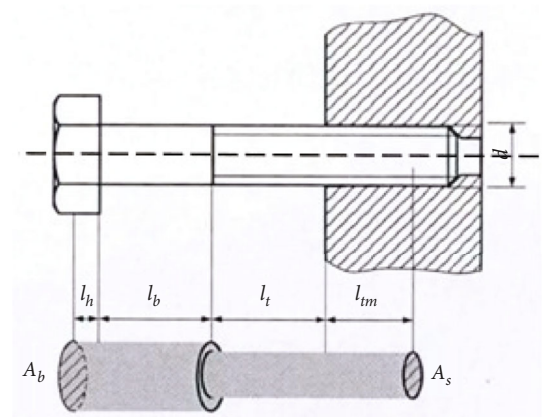

Figure 2: Simplified model of bolts.

According to the Euler-Bernoulli beam theory, the differential equations of motion for the two-degree-of-freedom bending deformation of this combined bolted beam structure can be developed as follows.

$$EI\frac{\partial^4 W_1(x,t)}{\partial^4 x} + m\frac{\partial^2 W_1(x,t)}{\partial^2 t} = F(t)\delta(x), \quad x \in (0, s), \tag{6}$$

$$EI\frac{\partial^4 W_2(x,t)}{\partial^4 x} + m\frac{\partial^2 W_2(x,t)}{\partial^2 t} = 0 \quad x \in (s, l), \tag{7}$$

where m, E, and I represent the mass per unit length, the modulus of elasticity, and the moment of inertia of the beam, respectively; $W_1(x,t)$ and $W_2(x,t)$ represent the transverse displacement of the two beams, respectively; and $F(t)$ represent the external load acting on the beam.

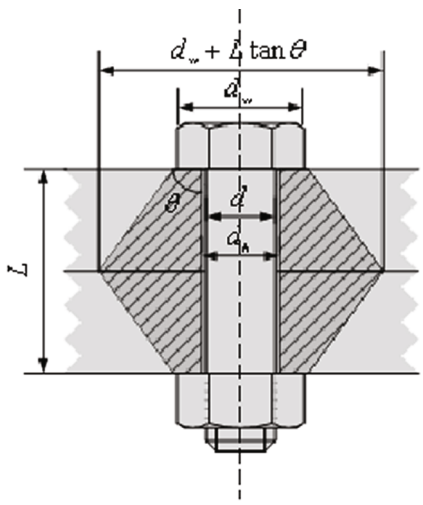

Figure 3: Figure of force area of coupled parts.

Considering the boundary conditions and the continuity conditions at the coupling, the fixed boundary conditions for this bolted coupling beam combination structure are

$$W_1(0,t) = \frac{\partial W_1(0,t)}{\partial x} = 0,$$
$$W_2(l,t) = \frac{\partial W_2(l,t)}{\partial x} = 0. \tag{8}$$

The shear force and bending moment are equal on both sides of the joint, i.e., at $x = s$, then

$$\frac{\partial^3 W_1(s,t)}{\partial x^3} = \frac{\partial^3 W_2(s,t)}{\partial x^3},$$
$$\frac{\partial^2 W_1(s,t)}{\partial x^2} = \frac{\partial^2 W_2(s,t)}{\partial x^2}. \tag{9}$$

Assuming K_l is the shear stiffness of the coupling part, it is obtained from the shear balance that

$$-EI\frac{\partial^3 W_1(s,t)}{\partial x^3} = K_l(W_2(s,t) - W_1(s,t)). \tag{10}$$

The nonlinear characteristics of the bolted joint are characterized by the linear torsional stiffness K_θ, the cubic term stiffness K_3 and the viscous damping coefficient C, which can be obtained from the bending equilibrium of the joint as follows:

$$EI\frac{\partial^2 W_1(s,t)}{\partial x^2} = C\left(\frac{\partial^2 W_2(s,t)}{\partial x\partial t} - \frac{\partial^2 W_1(s,t)}{\partial x\partial t}\right) + K_\theta\left(\frac{\partial W_2(s,t)}{\partial x} - \frac{\partial W_1(s,t)}{\partial x}\right) - K_3\left(\frac{\partial W_2(s,t)}{\partial x} - \frac{\partial W_1(s,t)}{\partial x}\right)^3. \tag{11}$$

3.2. Analytical Solution of Bolted Joint Beams Based on Multiscale Method. For the main resonant state near the linear first-order intrinsic frequency of a bolted beam structure, the external excitation can be considered as a small parameter term. According to the multiscale approach, making $F/m \longrightarrow \varepsilon f$, $C/m \longrightarrow \varepsilon\mu$, and $K_3/m \longrightarrow \varepsilon K_N$, Equation (6) and Equation (7) can be transformed into the follows:

$$\frac{EI}{m}\frac{\partial^4 W_1(x,t)}{\partial^4 x} + \frac{\partial^2 W_1(x,t)}{\partial^2 t} = \varepsilon f(t)\delta(x), \quad x \in (0,s), \tag{12}$$

$$\frac{EI}{m}\frac{\partial^4 W_2(x,t)}{\partial^4 x} + \frac{\partial^2 W_2(x,t)}{\partial^2 t} = 0 \quad x \in (s,l). \tag{13}$$

The solution of the differential equation of motion for a bolted joint beam structure is expressed in terms of different time scales, such as $T_0 = t$, $T_3 = \varepsilon^3 t$, then,

$$W_1(x,t;\varepsilon) = W_{10}(x,T_0,T_3) + \varepsilon^3 W_{13}(x,T_0,T_3), \tag{14}$$

$$W_2(x,t;\varepsilon) = W_{20}(x,T_0,T_3) + \varepsilon^3 W_{23}(x,T_0,T_3). \tag{15}$$

Substituting the linear analytical expressions (14) and (15) into Equation (6)–Equation (13) and separating the ε^0 and ε^3 terms, the differential equations of motion, boundary conditions, and continuity conditions at different time scales can be obtained for the main resonant state near the first order intrinsic frequency.

3.2.1. ε^0-Order Term. The differential equations of motion are as follows:

$$D_0^2 W_{10} + \frac{EI}{m}W_{10}^4 = 0,$$
$$D_0^2 W_{20} + \frac{EI}{m}W_{20}^4 = 0. \tag{16}$$

The boundary conditions are as follows:

$$W_{10}(0,T_0,T_1) = W_{10}{}'(0,T_0,T_1) = 0,$$
$$W_{20}(l,T_0,T_1) = W_{20}{}'(l,T_0,T_1) = 0. \tag{17}$$

The continuity conditions are as follows:

$$W_{10}{}'''(s,T_0,T_1) = W_{20}{}'''(s,T_0,T_1),$$
$$W_{10}{}''(s,T_0,T_1) = W_{20}{}''(s,T_0,T_1),$$
$$EIW_{10}{}'''(s,T_0,T_1) = -K_l(W_{20}(s,T_0,T_1) - W_{10}(s,T_0,T_1)),$$
$$EIW_{10}{}''(s,T_0,T_1) = K_\theta\left(W_{20}{}'(s,T_0,T_1) - W_{10}{}'(s,T_0,T_1)\right). \tag{18}$$

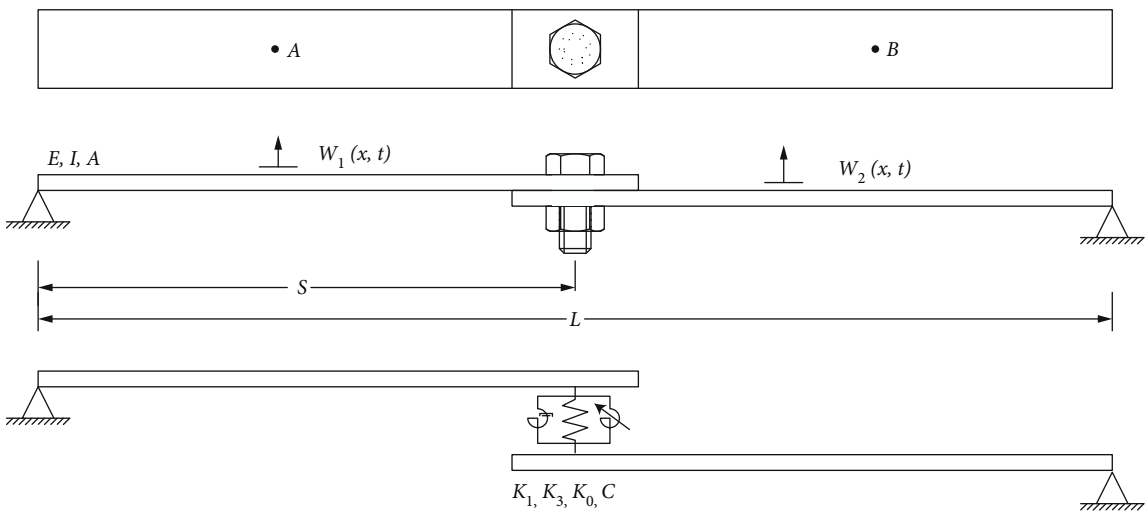

Figure 4: Bolt-on beams with fixed ends.

3.2.2. ε^3-Order Term. The differential equations of motion are as follows:

$$D_0^2 W_{13} + \frac{EI}{m} W_{13}^4 = f \cos(\Omega t)\delta(x) - 2D_0 D_1 W_{10}, \quad (19)$$

$$D_0^2 W_{23} + \frac{EI}{m} W_{23}^4 = -2D_0 D_1 W_{23}. \quad (20)$$

The boundary conditions are as follows:

$$\begin{aligned} W_{23}(0, T_0, T_3) &= W_{23}{}'(0, T_0, T_3) = 0, \\ W_{23}(l, T_0, T_3) &= W_{23}{}'(l, T_0, T_3) = 0. \end{aligned} \quad (21)$$

The continuity conditions are as follows:

$$\begin{aligned} W_{23}{}'''(s, T_0, T_2) &= W_{23}{}'''(s, T_0, T_3), \\ W_{23}{}''(s, T_0, T_3) &= W_{23}{}''(s, T_0, T_3), \\ EIW_{23}{}'''(s, T_0, T_3) &= K_l(W_{23}(s, T_0, T_3) - W_{23}(s, T_0, T_3)), \\ \frac{EI}{m} W_{23}{}''(s, T_0, T_1) &= \mu D_0\left(W_{20}{}'(s, T_0, T_1) - W_{10}{}'(s, T_0, T_1)\right) \\ &\quad + \frac{K_\theta}{m}\left(W_{23}{}'(s, T_0, T_3) - W_{11}{}'(s, T_0, T_3)\right) \\ &\quad - K_N\left(W_{20}{}'(s, T_0, T_3) - W_{10}{}'(s, T_0, T_3)\right)^3, \end{aligned} \quad (22)$$

where $(*)' = \partial/\partial x$, $\mathrm{d}/\mathrm{d}t = D_0 + \varepsilon D_1 + \varepsilon^2 D_2$, $\mathrm{d}^2/\mathrm{d}t^2 = D_0^2 + 2\varepsilon D_0 D_1 + \varepsilon^2(D_1^2 + 2\varepsilon D_0 D_2)$, and $D_n = \partial/\partial T$.

3.2.3. The First-Order Resonant Response of the ε^0-Order Term Homogeneous Equation. Assuming the form of its solution can be written as

$$W_{10}(x, T_0, T_3) = \left(A(T_3)e^{i\omega T_0} + \bar{A}(T_3)e^{-i\omega T_0}\right) Y_1(x), \quad (23)$$

$$W_{20}(x, T_0, T_3) = \left(A(T_3)e^{i\omega T_0} + \bar{A}(T_3)e^{-i\omega T_0}\right) Y_2(x), \quad (24)$$

where ω is the first-order intrinsic frequency of the structure, $\bar{A}(T_3)$ is the complex conjugate of the antecedent term, and $Y_i(x)$ is the oscillatory function of the first-order resonant response, which can be expressed as

$$Y_i(s) = \frac{1}{\sqrt{l}}\left(\cosh\frac{r_n s}{l} - \cos\frac{r_n s}{l} + \frac{\cos r_n + \cosh r_n}{\sin r_n + \sinh r_n}\left(\sin\frac{r_n s}{l} - \sinh\frac{r_n s}{l}\right)\right), \quad (25)$$

where r_n is the nth order root of the characteristic equation $1 + \cos(r)\cosh(r) = 0$.

Substituting Equation (23) and Equation (24) into the equation for the ε^0-order term yields

$$\begin{aligned} Y_1^4 - \lambda^4 Y_1 &= 0, \\ Y_2^4 - \lambda^4 Y_2 &= 0, \\ \lambda^4 &= \frac{m\omega^2}{\mathrm{EI}}, \\ Y_1(0) &= Y_1{}'(0) = 0, \\ Y_2(L) &= Y_2{}'(L) = 0, \\ Y_1{}'''(s) &= Y_2{}'''(s), \\ Y_1{}''(s) &= Y_2{}''(s), \\ EIY_1{}'''(s) &= -K_l(Y_2(s) - Y_1(s)), \\ EIY_1{}''(s) &= K_\theta\left(Y_2{}'(s) - Y_1{}'(s)\right). \end{aligned} \quad (26)$$

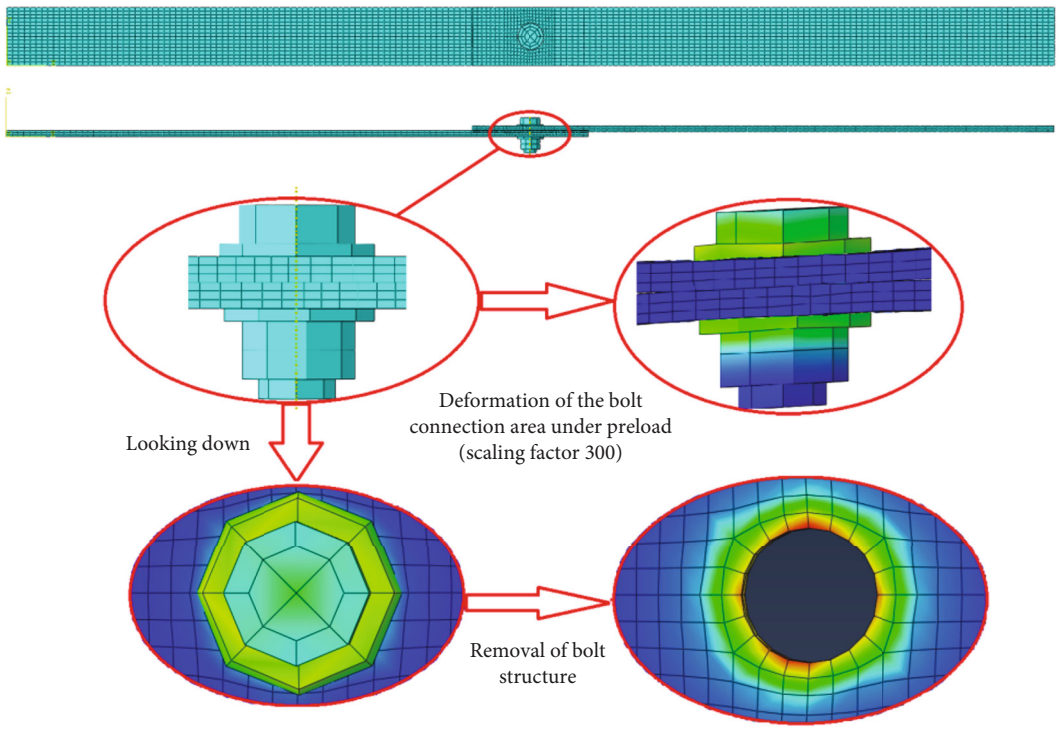

Figure 5: ABAQUS model for simulation tests.

Table 1: Test measurement frequency.

Order	1	2	3	4
Frequency (Hz)	20.629	79.812	125.06	232.15

3.2.4. The Solutions of Nonhomogeneous Equations of ε^3-Order Term. Substituting Equation (25) into Equation (19) and Equation (20) yields

$$D_0 W_{13} + \frac{EI}{m} W_{13}^4 = \frac{1}{2} f\delta(x) e^{i\Omega T_0} - 2i\omega Y_1 D_2 A e^{i\omega T_0}, \quad (27)$$

$$D_0 W_{13} + \frac{EI}{m} W_{13}^4 = -2i\omega Y_1 D_2 A e^{i\omega T_0}. \quad (28)$$

In this manuscript, the frequency of the external excitation Ω is assumed to be close to the first order natural frequency ω of the structure, i.e., $\Omega = \omega + \varepsilon^2\sigma$. where σ denotes the simple harmonic parameter and ε is the minor parameter.

Assuming that the amplitude A can be expressed in the following form:

$$A = \frac{1}{2}\rho e^{i(\sigma T_2 - \gamma)}. \quad (29)$$

Substituting Equation (29) into Equation (27) and Equation (28) and separating the real and imaginary parts, which yields

$$\begin{aligned} \rho' &= \frac{1}{2}\hat{f}\omega \sin\gamma, \\ \rho\gamma' &= \sigma\rho + \frac{1}{2}\hat{f}\omega \sin\gamma, \end{aligned} \quad (30)$$

where $\hat{f} = f\int_0^l Y_i(x)$.

Assuming that the solution to the system of equations consists of a long term φ_i and a nonlong term V_i.

$$\begin{aligned} W_{13}(x, T_0, T_1) &= \varphi_1(x, T_3)e^{i\omega T_0} + V_1(x, T_0, T_3) + \bar{A}(T_3)e^{-i\omega T_0}, \\ W_{23}(x, T_0, T_3) &= \varphi_2(x, T_3)e^{i\omega T_0} + V_2(x, T_0, T_3) + \bar{A}(T_3)e^{-i\omega T_0}. \end{aligned} \quad (31)$$

Substituting the solution to the equation for the ε^3-order term, so that the coefficients of the long-term terms on the left and right sides of the equation are equal, and thus eliminating the long term, can be further obtained as

$$\frac{\mathrm{EI}}{m}\left(\varphi_1^4 - \lambda^4\varphi_1\right) = \frac{f}{2}\delta(x)e^{i\sigma T_1} - 2i\omega Y_1 D_1 A, \quad (32)$$

$$\frac{\mathrm{EI}}{m}\left(\varphi_2^4 - \lambda^4\varphi_2\right) = -2i\omega Y_2 D_1 A. \quad (33)$$

Multiplying Equation (32) and Equation (33) by Y_1 and Y_2, respectively, and integrating along the direction x, the results can be summed as

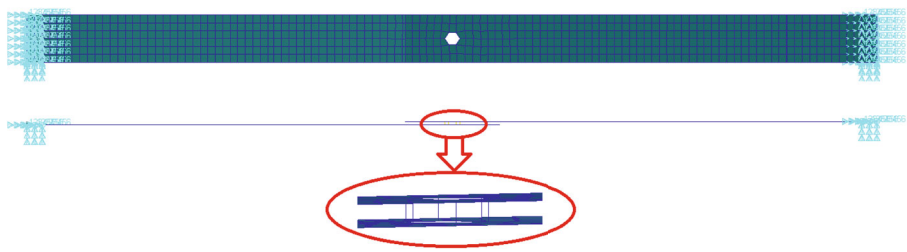

Figure 6: Finite element simulation calculation model.

Table 2: First 4th order natural frequency of the structure for the linearized equivalent of the bolt.

Order	1	2	3	4
Natural frequency (Hz)	23.082	81.378	129.38	239.11
Errors	11.89%	1.96%	3.45%	3.00%

$$\frac{EI}{m}\left(\int_0^s\left(\varphi_1^4 Y_1(x)-\lambda^4\varphi_1 Y_1(x)\right)\mathrm{d}x+\int_s^l\left(\varphi_2^4 Y_2(x)-\lambda^4\varphi_2 Y_2(x)\right)\mathrm{d}x\right)$$
$$=\int_0^s\left(\frac{f}{2}\delta(x)\mathrm{e}^{i\sigma T_1}Y_1(x)-2i\omega Y_1^2(x)D_1A\right)\mathrm{d}x+\int_s^l\left(-2i\omega Y_2^2(x)D_1A\right)\mathrm{d}x. \tag{34}$$

By divisional integration and introducing the boundary conditions and continuity conditions for the ε-order term and the ε^3-order term, the above equation can be transformed into

$$3K_N A^2\bar{A}\left(Y_2{}'(s)-Y_1{}'(s)\right)^4-i\omega\mu A\left(Y_2{}'(s)-Y_1{}'(s)\right)^2$$
$$+2\left(\frac{1}{3}(Y_2(s))^3-\frac{1}{3}(Y_1(s))^3\right)i\omega D_1A+\frac{f}{2}Y_1(s)\mathrm{e}^{i\sigma T_1}=0. \tag{35}$$

Making $p=(Y_2{}'(s)-Y_1{}'(s))^2$, $q=(1/3)(Y_2(s))^3-(1/3)(Y_1(s))^3$, then, the above equation can be further rewritten as

$$3K_N A^2\bar{A}p^2-i\omega\mu Ap+2i\omega qD_1A+\frac{f}{2}Y_1(s)\mathrm{e}^{i\sigma T_1}=0. \tag{36}$$

Therefore, the equation for the nonlinear frequency response function of the bolted beam structure can be expressed as

$$\begin{cases}\dfrac{\mu\rho p}{2q}=\dfrac{fY_1(s)}{2\omega q}\sin\gamma,\\[2ex] \rho\sigma+\dfrac{3K_N\rho^3p^2}{8\omega q}=-\dfrac{fY_1(s)}{2\omega q}\cos\gamma.\end{cases} \tag{37}$$

The equation for the first-order amplitude frequency resonance curve for a bolted jointed beam structure can be written as

$$\left[\left(\frac{\mu p}{2q}\right)^2+\left(\sigma+\frac{3K_N\rho^2p^2}{8\omega q}\right)^2\right]\rho^2=\left(\frac{fY_1(s)}{2\omega q}\right)^2. \tag{38}$$

The Equation (38) can be further rewritten as

$$\sigma=-\frac{3K_N\rho^2p^2}{8\omega q}\pm\sqrt{\left(\frac{fY_1(s)}{2\omega q\rho}\right)^2-\left(\frac{\mu p}{2q}\right)^2}. \tag{39}$$

According to the nature of the frequency response function, at the peak of the frequency response function meets the following:

$$\frac{fY_1(s)}{2\omega\rho^*}=\frac{\mu p}{2}, \tag{40}$$

$$\sigma^*=-\frac{3K_N(\rho^*)^2p^2}{8\omega q}. \tag{41}$$

where ρ^* and σ^* denote the response amplitude at the peak of the structural nonlinear frequency response function and the simple harmonic parameter.

From Equation (40) and Equation (41), we can further obtain that

$$C=\frac{fY_1(s)}{\omega\rho^*p}, \tag{42}$$

$$K_3=-\frac{8\omega mq(\Omega-\omega)}{3(\rho^*)^2p^2}. \tag{43}$$

Because the relatively small amplitude of changes in the nonlinear stiffness of bolted joints, the matrix perturbation method [13] can also be used to solve for the equivalent stiffness

$$K(K_l,K_\theta,K_3,C)=K(K_l,K_\theta,K_3,C)_0+\Delta K(K_l,K_\theta,K_3,C)_1. \tag{44}$$

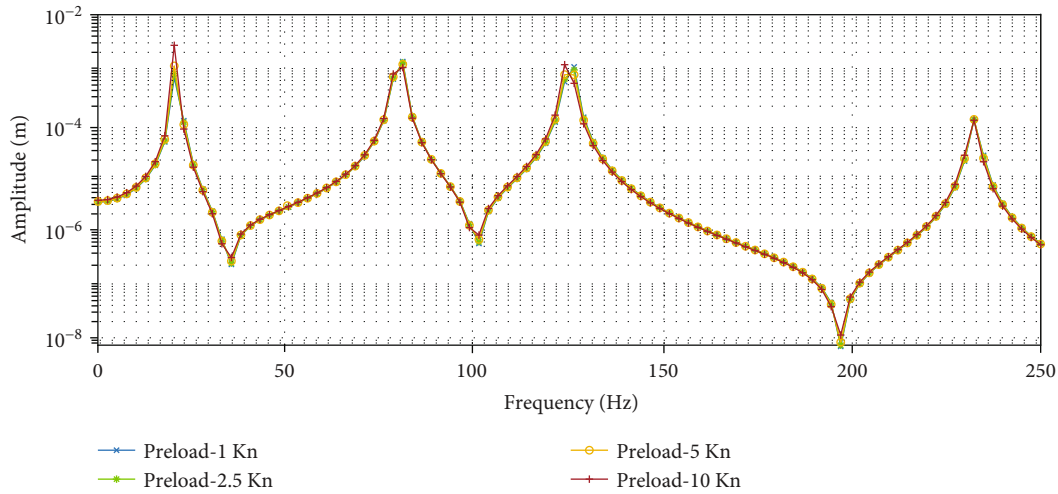

Figure 7: Linear frequency response function curves of bolted beam structures under different bolt preloads.

Table 3: First 4th order linear natural frequency of the structure under different bolt preloads.

		Linear natural frequency (Hz)			
		First order	Second order	Third order	Firth order
Bolt preloads (KN)	1	20.929	79.824	125.26	232.53
	2.5	20.865	79.795	125.17	232.46
	5	20.758	79.747	125.00	232.35
	10	20.545	79.656	124.68	232.12

where Δ is a small parameter, and the system corresponding to $\Delta = 0$ is called the original system, $K(K_l, K_\theta, K_3, C)_0$ is the equivalent stiffness of original system, and $\Delta K(K_l, K_\theta, K_3, C)_1$ denotes the variation.

According to perturbation theory, the eigenvector u and eigenvalues λ of the Equation (11) can be expanded into power series according to small parameters

$$\begin{cases} u^i = u_0^i + \Delta u_1^i + \Delta^2 u_2^i + \cdots, \\ \lambda^i = \lambda_0^i + \Delta \lambda_1^i + \Delta^2 \lambda_2^i + \cdots, \end{cases} \tag{45}$$

where λ_0^i and u_0^i are the eigenvalues and eigenvectors of the original system, λ_1^i and λ_2^i are the first and second order perturbations of eigenvalues, and u_1^i and u_2^i are the first- and second-order perturbations of eigenvectors, respectively.

According to the expansion theorem and the regularization condition, the approximate perturbation solutions of eigenvectors and eigenvalues can be obtained. This method has strong advantages in terms of computational speed and solution accuracy in engineering applications.

4. Numerical Validation of Equivalent Stiffness Modelling Methods for Bolted Joint Structures

In finite element analysis, contact conditions are a special type of discontinuous constraint that allows forces to be transmitted from one part of the model to another. When two surfaces come into contact, contact forces are generated. When the two surfaces separate, there is no constraint, making this constraint type discontinuous. Contact problems are highly nonlinear behaviors that require not only a significant amount of computational resources but also pose considerable difficulties during the modeling and assumption phase. In general, fundamental contact issues mainly focus on two aspects: firstly, the determination of the contact area, and secondly, the determination of frictional forces during contact.

In order to further illustrate the influence of traditional linear equivalent simulation and equivalent simulation considering nonlinear factors on the accuracy of simulation calculation in the process of finite element modelling calculation of bolted structure, this manuscript adopts ABAQUS, which is a finite element simulation analysis software with strong ability to deal with nonlinear problems, to carry out finite element modelling simulation calculation of bolted joint beam structure and simulate the real dynamic test results of the structure, the finite element model is shown in Figure 5. The bolted beam structure was fixed at both ends, and the nonlinear contact of the bolts was simulated by defining the friction coefficient and contact stiffness on each contact surface of the structure. The finite element model is modelled using the uncoordinated mode of the 8-node C3D8 3D stress cell, which on the one hand can accurately simulate the contact stresses and contact deformations at the bolt bond area and on the other hand can overcome the problem of scattered calculations due to shear locking

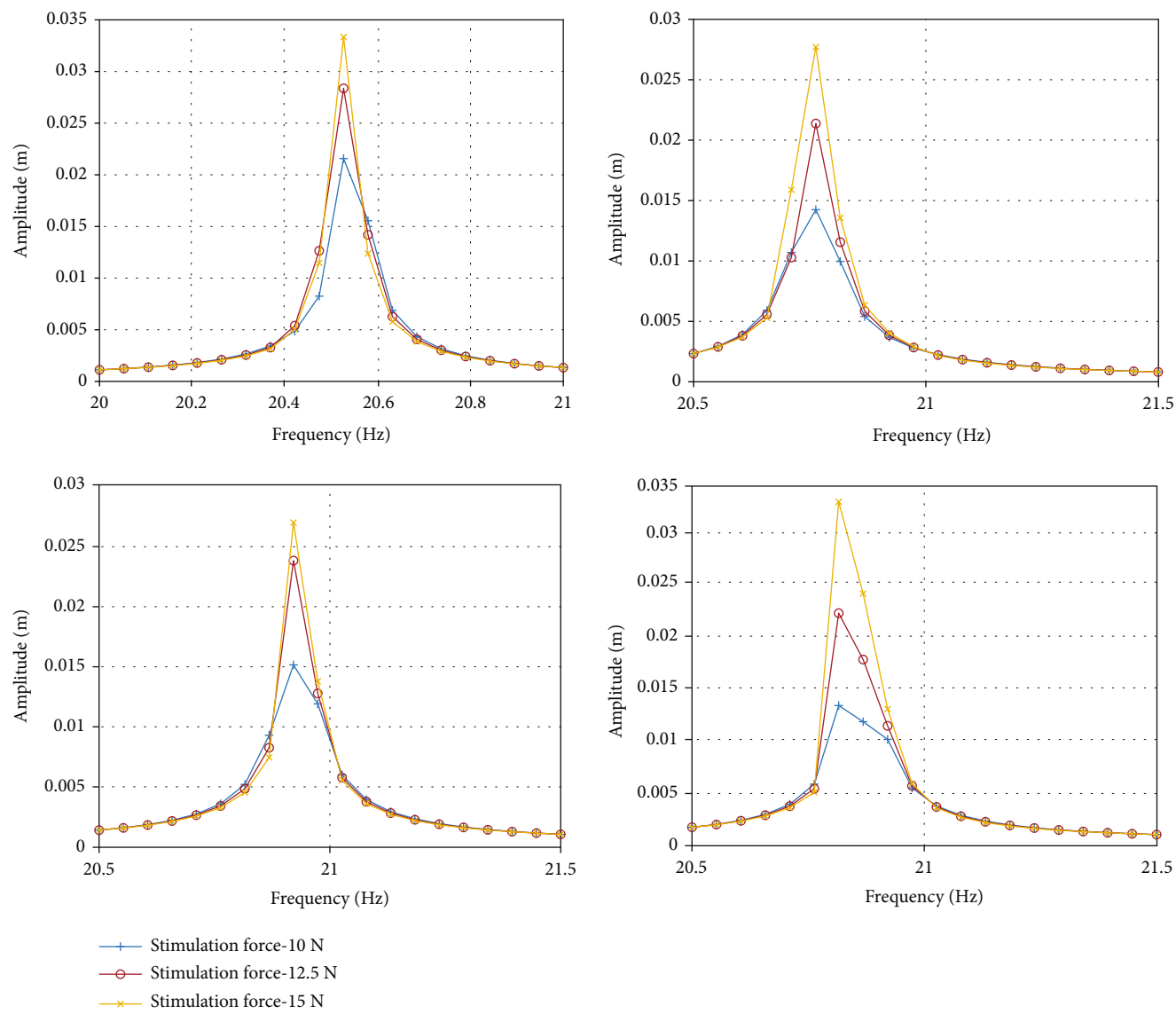

Figure 8: Frequency response function curves of bolted beam structures under different excitation forces.

Table 4: Kl and K_θ for different bolt preloads.

Bolt preloads	1KN	2.5KN	5KN	10KN
K_l(N/m)	5.227×10^4	5.207×10^4	5.169×10^4	5.098×10^4
K_θ(N/rad)	394.4	383.9	366.9	335.4

of fully integrated first-order cells. In addition, in order to make the ABAQUS simulation calculation results more realistic simulation of the dynamics test, this manuscript adds 5% white noise to the simulation calculation results to simulate the real test results, and the test measurement frequency as shown in Table 1.

4.1. Linearized Modelling Simulation and Equivalent Stiffness Calculation. Due to the solid meshes, nonlinear contact algorithms, and other factors, the ABAQUS-based finite element model described above is time-consuming and computationally inefficient. In order to improve calculation efficiency, beam units and shell units are usually used to simulate bolted coupling beams, and connection units are used to simulate bolts in practice. Then, in this part, the shell unit is used to simulate the bolted coupling beam, and the connection unit is used to simulate the bolts. The finite element model is shown in Figure 6.

The beam parameters are known as modulus of elasticity $E = 70$ Gpa, length $l = 0.5$ m, bolt position $S = 0.45$ m, density

Table 5: Nonlinear parameters of bolted beam structures under different excitation forces and bolt preloads.

Bolt preloads (KN)	Excitation force (N)	First-order peak frequency (Hz)	Displacement amplitude (m)	Damping coefficient C (Ns/m)	Cubic item stiffness K_3 (N/m^3)
1	10	20.921	0.01516	0.0414	1.528×10^4
	12.5	20.914	0.02384	0.0329	1.158×10^4
	15	20.907	0.02701	0.0348	1.324×10^4
2.5	10	20.816	0.01338	0.0476	8.818×10^4
	12.5	20.807	0.02223	0.0355	3.449×10^4
	15	20.798	0.03323	0.0285	1.657×10^4
5	10	20.763	0.01425	0.0448	1.142×10^5
	12.5	20.755	0.02138	0.0373	5.317×10^4
	15	20.747	0.03325	0.0288	2.299×10^4
10	10	20.526	0.02157	0.0396	1.210×10^5
	12.5	20.520	0.02837	0.0281	7.098×10^4
	15	20.514	0.03333	0.0287	5.218×10^4

Table 6: Parameter identification results for the bolted beam structure in various operating conditions.

	Stimulation force 10 N	Stimulation force 12.5 N	Stimulation force 15 N
Bolt preload 1 KN	$K_l = 5.227 \times 10^4$N/m	$K_l = 5.227 \times 10^4$N/m	$K_l = 5.227 \times 10^4$N/m
	$K_\theta = 394.4$N/rad	$K_\theta = 394.4$N/rad	$K_\theta = 394.4$N/rad
	$K_3 = 1.528 \times 10^4$N/m^3	$K_3 = 1.358 \times 10^4$N/m^3	$K_3 = 1.324 \times 10^4$N/m^3
	$C = 0.0414$Ns/m	$C = 0.0329$Ns/m	$C = 0.0248$Ns/m
Bolt preload 2.5 KN	$K_l = 5.207 \times 10^4$N/m	$K_l = 5.207 \times 10^4$N/m	$K_l = 5.207 \times 10^4$N/m
	$K_\theta = 383.9$N/rad	$K_\theta = 383.9$N/rad	$K_\theta = 383.9$N/rad
	$K_3 = 8.818 \times 10^4$N/m^3	$K_3 = 3.449 \times 10^4$N/m^3	$K_3 = 1.657 \times 10^4$N/m^3
	$C = 0.0476$Ns/m	$C = 0.0355$Ns/m	$C = 0.0285$Ns/m
Bolt preload 5 KN	$K_l = 5.169 \times 10^4$N/m	$K_l = 5.169 \times 10^4$N/m	$K_l = 5.169 \times 10^4$N/m
	$K_\theta = 366.9$N/rad	$K_\theta = 366.9$N/rad	$K_\theta = 366.9$N/rad
	$K_3 = 1.142 \times 10^5$N/m^3	$K_3 = 5.317 \times 10^4$N/m^3	$K_3 = 2.299 \times 10^4$N/m^3
	$C = 0.0448$Ns/m	$C = 0.0373$Ns/m	$C = 0.0288$Ns/m
Bolt preload 10 KN	$K_l = 5.098 \times 10^4$N/m	$K_l = 5.098 \times 10^4$N/m	$K_l = 5.098 \times 10^4$N/m
	$K_\theta = 335.4$N/rad	$K_\theta = 335.4$N/rad	$K_\theta = 335.4$N/rad
	$K_3 = 1.210 \times 10^5$N/m^3	$K_3 = 7.098 \times 10^4$N/m^3	$K_3 = 5.218 \times 10^4$N/m^3
	$C = 0.0396$Ns/m	$C = 0.0281$Ns/m	$C = 0.0187$Ns/m

$\rho = 2710$ kg/m^3, mass per unit length $m = 0.542$ kg/m, and moment of inertia $I = 2.67 \times 10^{-10}$ m^4. The bolts are standard hexagonal bolts of M12 and the nuts are standard hexagonal nuts of M12, and the parameters are known as modulus of elasticity $E = 209$ Gpa and density $\rho = 7890$ kg/m^3.

Substituting the geometric parameters of the bolt and the bolted coupling beam into Equation (2)–Equation (5), the equivalent stiffness of the linearized bolt is calculated as 1.1015×10^9 N/m. The first 4 orders of natural frequencies of the structure are calculated based on the FEM numerical simulation software and are shown in Table 2.

As we can see from the comparison in Table 2, the equivalent stiffness values obtained by the linearized equivalence method are larger and correspond to a completely rigid

Table 7: Bolt nonlinearized equivalent of the first 4th-order natural frequency of the structure.

	1st frequency/Hz error	2nd frequency/Hz error	3rd frequency/Hz error	4th frequency/Hz error
1KN-10 N	20.592	80.242	126.17	230.64
	0.179%	0.539%	0.888%	0.650%
1KN-12.5 N	20.588	79.923	126.14	230.64
	0.199%	0.139%	0.864%	0.650%
1KN-15 N	20.590	80.089	126.15	230.64
	0.189%	0.347%	0.872%	0.650%
2.5KN-10 N	20.636	80.025	126.51	230.51
	0.034%	0.267%	1.159%	0.706%
2.5KN-12.5 N	20.578	80.776	126.06	230.49
	0.247%	1.208%	0.780%	0.715%
2.5KN-15 N	20.558	80.776	126.06	230.49
	0.344%	0.640%	0.672%	0.715%
5KN-10 N	20.593	81.044	126.18	230.23
	0.175%	1.544%	0.900%	0.827%
5KN-12.5 N	20.540	80.920	125.76	230.21
	0.431%	1.388%	0.560%	0.836%
5KN-15 N	20.504	80.567	125.48	20.21
	0.606%	0.946%	0.336%	0.836%
10KN-10 N	20.479	81.044	125.30	229.68
	0.727%	1.544%	0.192%	1.064%
10KN-12.5 N	20.442	80.99	125.01	229.67
	0.906%	1.476%	0.040%	1.068%
10KN-15 N	20.417	80.915	124.83	229.67
	1.028%	1.382%	0.184%	1.068%

connection to the structure, which does not correspond to the actual structural connection. And the resulting calculated intrinsic frequencies of each order are greater than the experimental measurements, especially the first-order frequency error of about 12%. Since in engineering we tend to be more concerned with the lower-order modalities of a structure, obtaining a finite element model by linearized equivalence is not suitable for practical engineering.

4.2. Modelling Simulation and Equivalent Stiffness Calculation considering Nonlinear Factors. As linearized equivalence would lead to overly rigid structures with large frequencies, the effect of nonlinear factors needs to be considered to realistically and accurately simulate the bolted joint. In this manuscript, the modal analysis of the structure is carried out by applying a random excitation at the position of point A shown in Figure 7 and measuring the linear frequency response of the bolted beam structure at the position of point B to obtain the first four orders of linear natural frequencies of the structure. According to the strength limits of the bolts in the mechanical design manual, the modal frequencies of the structure were calculated for four working conditions, namely, 1 KN, 2.5 KN, 5 KN, and 10 KN for the preload force of the bolts. The curves of the linear frequency response function at point B for these four operating conditions are shown in Figure 7, and the frequency values corresponding to the first four resonance peaks of the linear frequency response function of the bolted beam for these four operating conditions are shown in Table 3.

Figure 8 shows the displacement frequency response function curves of the bolted beam structure in the frequency range around the peak of the first-order resonance, which taking different magnitudes of bolt preload and different magnitudes of excitation force account.

4.2.1. Linear Term Parameter Identification. Substituting the geometric and physical parameters of the bolted beam structure into Equation (37), we can obtain a system of equations for the vibration function coefficients A_i, B_i, C_i, and D_i. By making the rank of the determinant of this equation equal to 0, we can obtain a quadratic equation for shear stiffness K_l and torsional stiffness K_θ. According to the values of the first 4 orders of natural frequencies of the structure for the 4 operating conditions in Table 4, a system of 4 equations for K_l and K_θ can be obtained. Solving the system of equations further gives the sums for the bonded parts of the bolted beam structure, as shown in Table 4.

4.2.2. Nonlinear Term Parameter Identification. Substituting the linear term parameters of the bolted beam structure into Equation (37), we can obtain a system of equations for the vibration function coefficients A_i, B_i, C_i, and D_i. Then the vibration functions of the bolted beam structure at first-

order resonant frequencies for the above four working conditions are as follows:

Under a preload force of 1 KN for the bolts:

$$\begin{cases} Y_1(x) = 0.1406 \sin(4.734x) - 0.1592 \cos(4.734x) - 0.1406 \sinh(4.734x) + 0.1592 \cosh(4.734x), \\ Y_2(x) = 0.2046 \sin(4.734x) - 0.0569 \cos(4.734x) - 0.6554 \sinh(4.734x) + 0.6596 \cosh(4.734x). \end{cases} \tag{46}$$

Under a preload force of 2.5 KN for the bolts:

$$\begin{cases} Y_1(x) = 0.1394 \sin(4.726x) - 0.1582 \cos(4.726x) - 0.1395 \sinh(4.726x) + 0.1582 \cosh(4.726x), \\ Y_2(x) = 0.2036 \sin(4.726x) - 0.055 \cos(4.726x) - 0.6561 \sinh(4.726x) + 0.6604 \cosh(4.726x). \end{cases} \tag{47}$$

Under a preload force of 5 KN for the bolts:

$$\begin{cases} Y_1(x) = 0.1376 \sin(4.714x) - 0.1565 \cos(4.714x) - 0.1376 \sinh(4.714x) + 0.1565 \cosh(4.714x), \\ Y_2(x) = 0.2018 \sin(4.714x) - 0.0518 \cos(4.714x) - 0.6573 \sinh(4.714x) + 0.6616 \cosh(4.714x). \end{cases} \tag{48}$$

Under a preload force of 10 KN for the bolts:

$$\begin{cases} Y_1(x) = 0.134 \sin(4.69x) - 0.1534 \cos(4.69x) - 0.134 \sinh(4.69x) + 0.1534 \cosh(4.69x), \\ Y_2(x) = 0.1985 \sin(4.69x) - 0.0457 \cos(4.69x) - 0.6595 \sinh(4.69x) + 0.6637 \cosh(4.69x). \end{cases} \tag{49}$$

According to Equation (42) and Equation (43), it can be seen that when the bolt preload and the excitation force are determined, the amplitude of the frequency response function of a bolted beam structure is determined by the damping factor C, and the frequency shift of the frequency response function is determined by the square term stiffness K_3. Therefore, from Equation (46) to Equation (49), the corresponding nonlinear parameters of the bolted beam structure for different excitation forces and bolt preloads can be further obtained, as shown in Table 5.

Therefore, when the preload force of the bolt was 1 KN, 2.5 KN, 5 KN, 10 KN, respectively, and the excitation force was 10 N, 12.5 N, 15 N, respectively, the identified K_l, K_θ, K_3 and C under each working condition were shown in Table 5. According to the identified parameters K_l and K_θ and finite element simulations, the simulation frequencies of the equivalent model of the bolted beam structure considering the influence of nonlinear factors are shown in Table 6.

It can be seen from Table 6, K_l and K_θ are independent of the magnitude of the excitation force and are related to the amount of bolt preload, which decreases as the bolt preload increases. K_3 is related to the excitation force and the bolt preload, generally decreasing with increasing excitation force and increasing with increasing bolt preload. Then, the bolted beam structure in this example has soft characteristics, and the resonance frequency decreases with increasing excitation level, which agrees with the results in Table 7.

As it can be seen from Table 7, the simulation calculations consider different excitation forces and bolt preloads for K_l, K_θ, K_3, and C. The maximum error between the simulation results and the test results for each working condition does not exceed 1.5%, which has a very high calculation accuracy. And in general, the accuracy of the bolted joint equivalence calculation, which considers the influence of nonlinearities, is much higher than that of the linearized equivalence calculation. Although the equivalence calculation process is relatively complex, the results are highly accurate and more in line with actual engineering conditions.

5. Conclusion

In this manuscript, an equivalent calculation method considering the influence of nonlinear factors for the bolted joint is proposed.

(1) A two-degree-of-freedom nonlinear dynamics model for a bolted beam structure with two solidly supported ends is developed, considering the nonlinear characteristics of the bolted joint structure, and cubic nonlinear stiffness and viscous damping are introduced to characterize the nonlinear characteristics of the bolted joint part

(2) According to the multiscale method, the corresponding analytical solutions for the nonlinear frequencies of the bolted joint beams of ε^0 order and ε^3 order are used, on the basis of which a reasonable identification of the linear and nonlinear model parameters can be achieved

(3) The validity and accuracy of the bolt nonlinear equivalent calculation method proposed in this manuscript are verified by a finite element simulation example of a bolted beam structure with fixed constraints at both ends

Data Availability

The data used to support the findings of this study are included within the article.

Conflicts of Interest

No potential conflict of interest was reported by the authors.

Acknowledgments

This research is supported by the Aviation Science Foundation of China (20200057052006). Besides, this research is a project Funded by the Priority Academic Program Development of Jiangsu Higher Education Institutions (PAPD).

References

[1] B. R. Kirby, "The behaviour of high-strength grade 8.8 bolts in fire," *Journal of Constructional Steel Research*, vol. 33, no. 1-2, pp. 3–38, 1995.

[2] C. J. Hartwigsen, *Dynamics of Jointed Beam Structures: Computational and Experimental Studies*, University of Illinois at Urbana-Champaign, 2002.

[3] D. Čelič and M. Boltežar, "Identification of the dynamic properties of joints using frequency-response functions," *Journal of Sound and Vibration*, vol. 317, no. 1-2, pp. 158–174, 2008.

[4] Ş. Tol and H. N. Özgüven, "Dynamic characterization of structural joints using FRF decoupling," in *Topics in Modal Analysis I, Volume 5*, pp. 435–446, Springer, New York, NY, USA, 2012.

[5] T. Yang, S. H. Fan, and C. S. Lin, "Joint stiffness identification using FRF measurements," *Computers & Structures*, vol. 81, no. 28-29, pp. 2549–2556, 2003.

[6] H. Ahmadian, J. E. Mottershead, S. James, M. I. Friswell, and C. A. Reece, "Modelling and updating of large surface-to-surface joints in the AWE-MACE structure," *Mechanical Systems and Signal Processing*, vol. 20, no. 4, pp. 868–880, 2006.

[7] K. Mao, B. Li, J. Wu, and X. Shao, "Stiffness influential factors-based dynamic modeling and its parameter identification method of fixed joints in machine tools," *International Journal of Machine Tools and Manufacture*, vol. 50, no. 2, pp. 156–164, 2010.

[8] D. J. Segalman, T. Paez, D. Smallwood, H. Sumali, T. Paez, and A. Urbina, *Status and Integrated Road-Map for Joints Modeling Research*, Sandia National Laboratories, Albuquerque, NM, Mexico, 2003.

[9] H. Jalali, H. Ahmadian, and J. E. Mottershead, "Identification of nonlinear bolted lap-joint parameters by force-state mapping," *International Journal of Solids and Structures*, vol. 44, no. 25-26, pp. 8087–8105, 2007.

[10] M. Iranzad and H. Ahmadian, "Identification of nonlinear bolted lap joint models," *Computers & Structures*, vol. 96-97, pp. 1–8, 2012.

[11] M. H. Mayer and L. Gaul, "Segment-to-segment contact elements for modelling joint interfaces in finite element analysis," *Mechanical Systems and Signal Processing*, vol. 21, no. 2, pp. 724–734, 2007.

[12] Q. Datong and X. Liyang, *Modern Machinery Handbook, vol. 6*, Chemical Industry Press, 2011.

[13] C. Liu, X. Yue, K. Shi, and Z. Sun, *Spacecraft Attitude Control: A Linear Matrix Inequality Approach*, Elsevier, 2022.